*International Journal of Engineering & Technology*, 7 (4) (2018) 3022-3025

International Journal of Engineering & Technology

*Website: www.sciencepubco.com/index.php/IJET*
*doi: 10.14419/ijet.v7i4.14884*
***Research paper***

# Temperature analysis of ZnO/p-Si heterojunction using thermionic emission model

**H. Hasim [1], S. M. Sultan [2] *, A. Mohamad [2]**

[1] *Malaysia Nuclear Agency, Bangi, Kajang, Selangor, Malaysia*
[2] *School of Electrical Engineering, Faculty of Engineering, University Teknologi Malaysia, Skudai, Johor, Malaysia*
**Corresponding author E-mail: suhanasultan@utm.my*

**Abstract**

Two ZnO/p-Si heterojunction diode structures are modeled based on thermionic emission in numerical computation environment, and their current-voltage characteristics were validated in Spice with 500 Ω and 5 kΩ load resistance. Both structures are differentiated based on thickness, metal size, and doping concentration. Parameters extracted such as barrier height, ideality factor, activation energy, series resistance, and shunt resistance are studied towards temperature-dependent study from 300 K to 673 K. Structure 1 proved to be exhibiting lower barrier height , series resistance and shunt resistance while structure 2 has lower ideality factor, activation energy, and turn on voltage. Modeling the ideality factor of structure 2 predicts a value of 0.25 at 673 K. Meanwhile, the turn on voltage of structure 2 is shown to achieve 0.8 V at room temperature. Barrier heights for structure 1 are reported to increase from 0.68 eV to 1.17 eV when temperature varies from 300 K to 673 K but series resistance and shunt resistance decreases with temperature.

***Keywords***: *Diode; radiation hard; Temperature; Thermionic Emission, ZnO/p-Si Heterojunction.*

## 1. Introduction

High temperature applications such as nuclear power plant, oil, and gas industry, and electric generation plants require the ability to withstand more than 373 K. Wide band gaps materials like SiC and ZnO have proven to operate at high temperatures [1-3]. Zinc Oxide (ZnO) is one of the promising material for semiconductor device applications. ZnO also has sizeable free exciton binding energy [4], wide band gap, high electron mobility, excellent transparency, high thermal conductivity, mechanically stable, large saturation velocity, excitonic emission process above room temperature, and stable radiation hardness [4]. In addition, it is available in bulk single crystal. Besides, it exhibits excellent design and fabrication process; it also performs well in wet chemical etching with low growth cost. Almost all ZnO exhibits n-type that spark an extensive debate and research. There are few ZnO heterojunction devices which have been reported such as $SrCu_2O_2$/ZnO [5], NiO/ZnO [6], ZnO/SiC [6], $ZnRh_2O_4$/ZnO [6] and ZnO/Si [4]. Nevertheless, ZnO/Si-based heterojunction device is the most studied due to its cost-effectiveness in fabrication and the maturity of Si-based material. ZnO based devices are studied for various electronic applications such as UV astronomy, sensors, light emitting diodes, piezoelectric, solar cell, actuator, space to space communication and environmental monitoring [7, 8, 9]. However, there is lack of study on ZnO material as semiconductor radiation detector. Currently, an excellent commercial radiation detector on the market is based on scintillation detector (inorganic scintillator), but this detector requires an additional cooler to operate at high temperature and bulky in size. ZnO electronic properties such as vast band gap exhibit good radiation absorption efficiency towards gamma and photon. The capability of a device to work in high radiation corresponds with the ability of the device to withstand high temperatures. There are many studies which investigate the ZnO device properties at high temperatures. However, the maximum temperature of these works is only up to 423K. There is very few research has been carried out to find the thermally stable structure that can be operated at temperature up to 673 K, which is the maximum temperature that a radiation detector should withstand. Combining the advantage of radiation hardness with the ability to operate at high temperatures make the ZnO as a suitable candidate to operate at high temperature applications. This work investigates the effect of various temperatures up to 673 K on ZnO/p-Si junction characteristics. Also, two types of structures will be analyzed based on their electrical characteristics and thermal stability of the device.

## 2. Modeling and simulation

Two types of heterojunction diode structures are identified to acquaint theory behind heterojunction diode, and it is ohmic contact. Both of these structures are taken from [6] for structure 1 and [10] for structure [2] and will be modeled based on thermionic emission as illustrated on Fig. 1. Some of the experimental data are taken from [6] and [10] respectively as semi-empirical modeling and analysis. Applying the numerical analysis, the modeling and analysis data are compared between structure 1 and structure 2 until it reached 673 K.

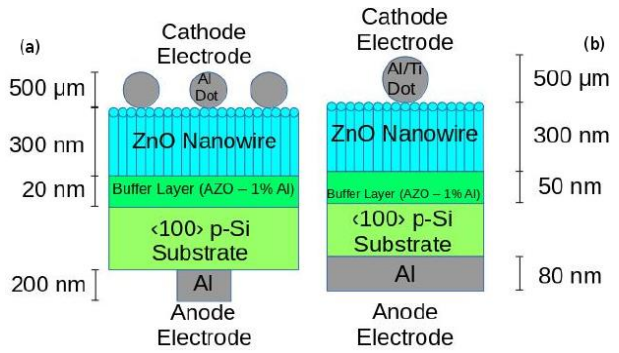


**Fig. 1:** Illustration of ZnO/p-Si Heterojunction Diode. A) Structure 1 and B) Structure 2.

Acceptor concentration $N_a$ and donor concentration $N_d$ need to be calculated based on experimental parameters obtained such as $V_{do}$ diffusion voltage, $V_{bi}$ built-in voltage, $m_e$ effective mass, and $n_c$ conduction band density of state as shown below.

$$m_{e(\text{DOS for ZnO})} = 0.27 m_{Oe} \tag{1}$$

$$m_{e(\text{DOS for p-Si})} = 1.08 m_{Oe} \tag{2}$$

where $m_O$ is the electron mass. Based on Eq(1) and Eq(2), the conduction band density of states, $n_c$ can be obtained as below.

$$n_{c(ZnO)} = \left[\frac{2\pi m_{e(\text{DOS for ZnO})} KT}{h^2}\right]^{1.5} \times 2 \tag{3}$$

$$n_{c(p-Si)} = \left[\frac{2\pi m_{e(\text{DOS for p-Si})} KT}{h^2}\right]^{1.5} \times 2 \tag{4}$$

where K, T, and q is the Boltzmann constant, temperature, and electron charge, respectively. Eq(5) shows the barrier height, ∅ value that can be found by including Eq(3).

$$\emptyset = V_{do} + \frac{KT}{q}\log\left(\frac{n_c(DOS\ for\ ZnO)}{n_d}\right) \tag{5}$$

where $V_{do}$ is the diffusion voltage which can be found from Eq (6). By replacing the barrier height value with the experimentally obtained, the acceptor, $n_a$ and donor concentration, $n_d$ can be found.

$$V_{do} = V_{bi} + \left(\frac{KT}{q}\right) \tag{6}$$

where

$$V_{bi} = \Delta E_c + 8.62\times10^{5} T\ \log\left(\frac{n_a n_d n_{c(\text{DOS for p-Si})}}{n_{i(p-Si)}^2 n_{c(\text{DOS for ZnO})}}\right) \tag{7}$$

where $\Delta E_C$ the conduction band offset which is the differences of conduction band energy or differences of electron affinity between ZnO and p-Si.

## 3. Analysis and discussion

Figure 2 shows a plot of barrier height against temperature from 300 K to 673 K for both structures. Structure 1 produces lower barrier height compare to structure 2. Structure 1 is also less affected by temperature change since the slope of barrier height towards temperature change of structure 1 and structure 2 are $1.29\text{x}10^{-3}$ eV/K and $1.45\text{x}10^{-3}$ eV/K respectively. The barrier height obtained from Structure 1 at room temperature is 0.68 eV which is close to 0.7 eV reported in [11].

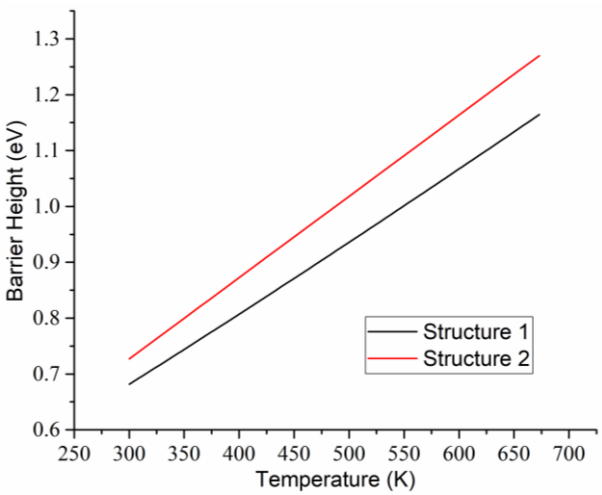


**Fig. 2:** Barrier Height of Structure 1 and Structure 2 against Temperature.

Furthermore, Fig. 3 defined the ideality factor of both structures toward temperature change. Structure 1 is more superior compare to structure 2 in term of ideality factor changing rate toward temperature change, that is $3.75\text{x}10^{-3}$ ideality factor over 1 K temperature change for structure 1 and $4.96\text{x}10^{-3}$ ideality factor over 1 K temperature change for structure 2. Since structure 2 reach ideality factor of 1 at 530 K thus it is better for application below than 530 K. Meanwhile, Yakuphanoglu et al. [12] and He et al. [13] obtain 3.2 and 2.5 ideality factor at room temperature which is close to structure 1 at 3.5 and structure 2 at 2.08.

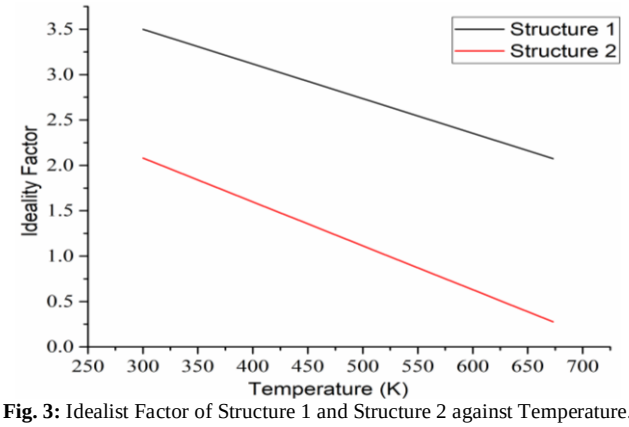


**Fig. 3:** Idealist Factor of Structure 1 and Structure 2 against Temperature.

Activation energy is derived from Arrhenius plot in Fig. 4. There is a gap of $1\text{x}10^{-4}$ eV between both structures. Equation(8) shows the relationship of $I_O$, reverse saturation current against temperature,T.

$$\ln(I_o) = \frac{E_a}{R}\frac{1}{T} - \ln(C) \tag{8}$$

where $E_a$ is the activation energy, R universal gas constant, and C intersection of the y-axis. From Equation (8), $E_a$ is initiated from the slope of the Arrhenius plot and found to be 0.3702 eV for structure 2 and 0.3703 eV for structure 1. This slight distinction of activation energy is because of small gap difference between structure 1 and structure two barrier height that affected reverse saturation current as in Equation (9).

$$I_o = AA^* T^2 \ln\left(\frac{-q\phi}{KT}\right) \tag{9}$$

where A and $A^*$ are the contact area and Richardson constant, respectively.

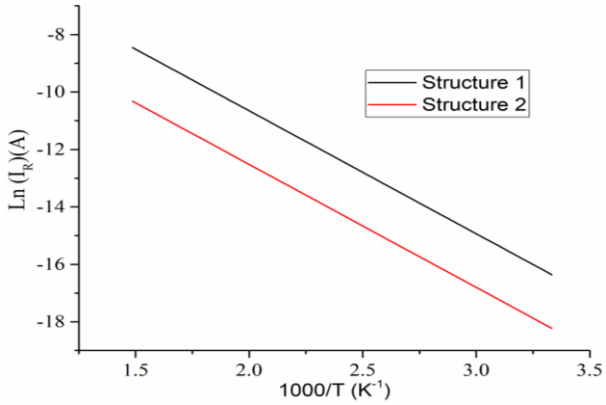


**Fig. 4 :** Arrhenius Plot of Structure 1 and Structure 2

Badran et al. [4] reported 0.2830 eV of activation energy which is a bit less compared to this modeling activation energy. This is because of the different structure will produce different volume and different conduction band density of state that affects the built- in potential, barrier height, reverse saturation current, and activation energy.

Fig.5 shows the plot of barrier height against the ideality factor for both structures. When there is a linear relationship between barrier height and ideality factor, it indicates barrier height irregularity as mentioned by Schmitsdorf et al. [14] in their device.

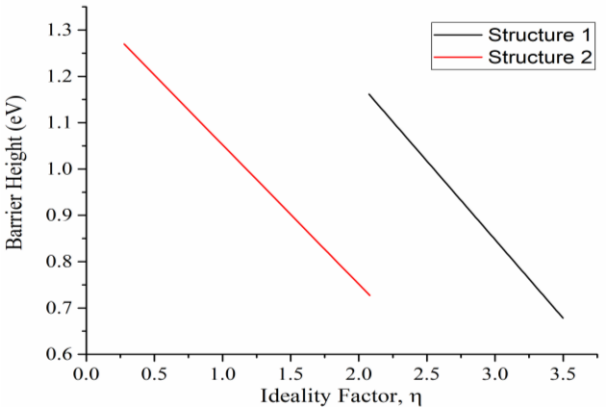


**Fig. 5:** Linearly Variation of Barrier Height and Ideality Factor toward Temperature.

The zero bias barrier height for structure 2 (1.35 eV) is less than structure 1 (1.87 eV). In addition, Structure 2 exhibits high current as it reaches below ideality factor equals 1, $\eta < 1$. This can be described below on thermionic emission current Equation (10).

$$I = I_o\left[\exp\left(\frac{V}{\eta V_T}\right)-1\right] \tag{10}$$

where V assign to a bias voltage, $\eta$ as ideality factor, and $V_T$ as thermal voltage.

Increasing temperature will project a decline of ideality factor and increases the current rapidly as shown in Fig. 6. Current of structure 2 exponentially rise higher compare to structure 1 at 673 K.

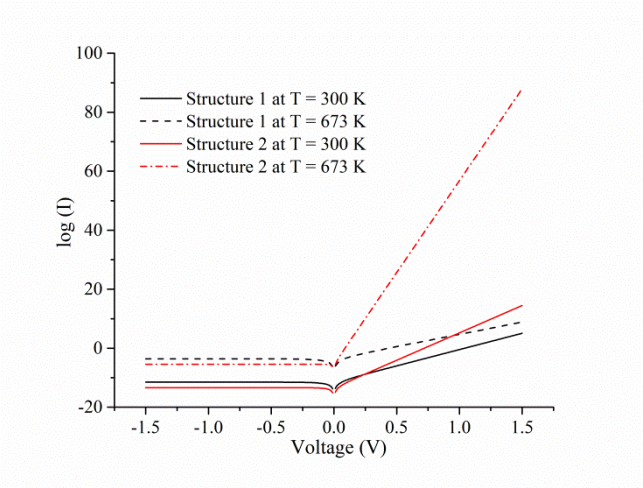


**Fig. 6:** Current Voltage Characteristics.

Series and shunt resistance is extracted from junction resistance against forward and reverse bias voltage. The series resistance that was extracted from junction ZnO and p-Si is 1700 Ω for structure 1. This value approximately close to 1610 Ω as reported in Aksoy et al. [15]. Meanwhile, shunt resistance that elucidates as the resistance between Al/p-Si and Al/ZnO found to be $1.05 \times 10^8$ Ω for structure 1. Both series and shunt resistance decreases when temperature increases as presented in Fig. 7.

ZnO/p-Si heterojunction diode is remodeled using Spice at room temperature to verify its current-voltage characteristic and diode behavior. Fig. 8 shows the circuit diagram. The parameters from structure 1 and structure 2 are compared such as the barrier height and ideality factor towards its effects in temperature variations, activation energy, and zero bias barrier height. Apart from that, current-voltage curve, series resistance, shunt resistance are also analyzed. Both load resistance of 500 Ω and 5 kΩ are used to model ZnO/p-Si heterojunction diode. The results are compared with results obtained from the semi-empirical model. Diode current-voltage validation is done on circuit simulation as shown in Fig. 9. Turn on voltage at room temperature for structure 1 and structure 2 are 0.8 V and 1.1 V (intersection between x-axis and straight line on Fig. 9), respectively. This value is almost similar to Klason et al. [16] device which achieved 1.1 V. While piecewise linear model resistance is 0.18 Ω and 0.35 Ω for structure 2 and structure 1 (straight line in Fig. 9), respectively. Structure 2 exhibits lower turn on voltage compared to Structure 1. Current-Voltage characteristic of structure 1 and structure 2 at 500 Ω and 5 kΩ load resistance on Spice been plotted in Fig. 9 as described in Equation (11) below.

$$V_S = V_{ON} + I_D r_D + I_D R_L \tag{11}$$

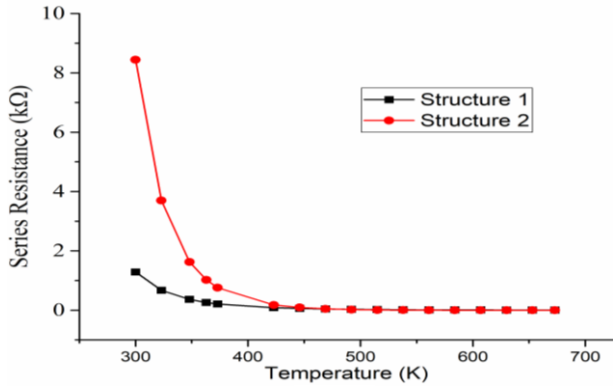


(a)

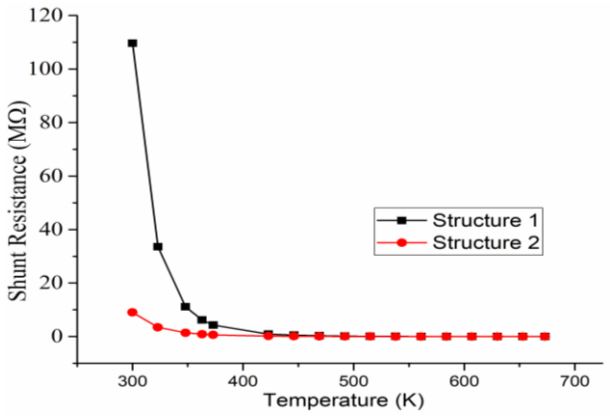


(b)

**Fig.7:** a) Series Resistance for both Structures when temperature increases and b) Shunt Resistance for both Structurse when temperature increases.

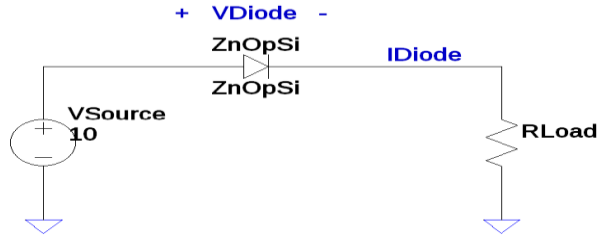


**Fig. 8:** Spice ZnO/p-Si Heterojunction Diode Model Simulation Circuit.

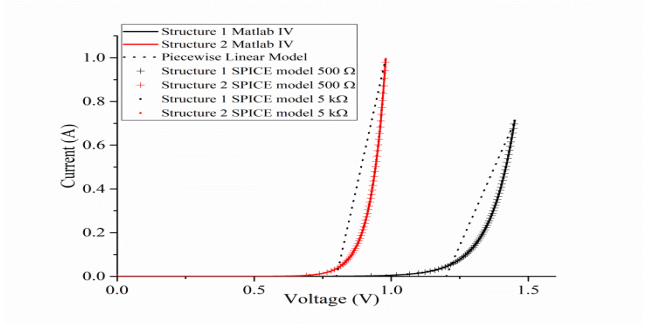


**Fig. 9:** Spice with Load Resistances and Numerical Computing Current-Voltage Characteristic.

## 4. Conclusions

Two types of structure ZnO/p-Si heterojunction diode has been modeled on the computational environment and verified its current-voltage characteristics on Spice simulation with 500 Ω and 5 kΩ load resistance. The barrier height of Structure 1 is 0.68 eV and exhibits less influence on temperature change which was found to be $1.29 \times 10^{-3}$ eV/K. Structure 1 unveils low series resistance and high shunt resistance at 1700 Ω and $1.05 \times 10^{8}$ Ω in which can reach ideality factor of 2.08 at 673 K. Meanwhile structure 2 has low turn on voltage, low activation energy and low piecewise linear model resistance at 0.8 V, 0.3702 eV and 0.18 Ω respectively. Structure 2 can reach an ideality factor less than 1, which in return will yield to the high current application since current multiplied exponentially as ideality factor less than 1.

## Acknowledgements

H. Hasim would like to thank Azriyani. M. Y for technical assistant. This study has been thoroughly sponsoring by Malaysia Public Service Department and Malaysia Nuclear Agency for the opportunity given to continue study. S. M. Sultan would like to acknowledge Research University Grant GUP Tier 1, Vote no. 14H63 and 19H33 for the research and financial support.

## References

[1] Ya. Ya. Kudryk, V. V. Shynkarenko1, V. S. Slipokurov, R. I. Bigun, and R. Ya. Kudryk, *Determination of the Schottky barrier height in diodes based on Au–$TiB_2$–n-SiC 6H from the current-voltage and capacitance-voltage characteristics*, Semiconductor Physics, Quantum Electronics & Optoelectronics 17 (2014) 398–402. https://doi.org/10.15407/spqeo17.04.398.

[2] Sofiienko. Andrii, Degoda. Volodymyr, Ponce-Marquez. David. M and Johansen. Geir. A, *Evaluation of monocrystalline ZnSe as a high-temperature radiation detector*, in 11th European Conference on Non-Destructive Testing (ECNDT 2014) (Prague, Czech Republic, 2014).

[3] Alvi. N. H, Riaz. M, Tzamalis. G, Nur. O and Willander. M, *Junction temperature in n-ZnO Nano rods/ (p-4H–SiC, p-GaN, and p-Si) heterojunction light emitting diodes*, Solid-State Electronics 54(2010) 536–540. https://doi.org/10.1016/j.sse.2010.01.020.

[4] Badran. R. I, Umar. Ahmad, Al-Heniti. S, Al-Hajry. A and Al-Harbi. T, *Synthesis and characterization of zinc oxide nanorods on silicon for the fabrication of p-Si/n-ZnO heterojunction diode*, Journal of Alloys and Compounds 508 (2010), 375–379. https://doi.org/10.1016/j.jallcom.2010.08.048.

[5] Chirakkara. Saraswathi and Krupanidhi. S. B, *Study of n-ZnO/p-Si (100) thin film heterojunctions by pulsed laser deposition without buffer layer*, Thin Solid Films 520 (2012), 5894–5899. https://doi.org/10.1016/j.tsf.2012.05.003.

[6] Sharma. Shashikant, and Periasamy. C, *A study on the electrical characteristic of n-ZnO/p-Si heterojunction diode prepared by vacuum coating technique*, Superlattices and Microstructures 73(2014), 12–21. https://doi.org/10.1016/j.spmi.2014.05.011.

[7] Masaud. T M Ben, Jaberansary. E, Sultan. S M, Clark. O, Sharp. T, Gunn. R, Bagnall. D M and Chong. H M H, *Compact Fabry-Perot electro-optic switch based on n-ZnO/p-Si heterojunction structure*, IEEE International Conference on Nanotechnology 1–3 (2012).

[8] WH. Khoo and SM. Sultan, *A study on the gas sensing effect on current-voltage characteristics of ZnO nanostructures*, International Conference on Semiconductor Electronics (ICSE2014), 221–224 (2014).

[9] SM. Sultan, K. Sun, MRR. De. Planque, P. Ashburn, and HMH. Chong, *Top-down fabricated ZnO nanowire transistors for application in biosensors*, 2012 Proceedings of the European Solid-State Device Research Conference (ESSDERC) 137–140 (2012).

[10] Somvanshi. Divya and Jit. S, *Analysis of Temperature-Dependent Electrical Characteristics of n-ZnO Nanowires (NWs)/p-Si Heterojunction Diodes*, IEEE Transactions on Nanotechnology 13(2014), 62–69. https://doi.org/10.1109/TNANO.2013.2290553.

[11] Pietruszka. R, Luka. G, Witkowski. B. S, Kopalko. K, Zielony. E, Bieganski. P, Placzek-popko. E, and Godlewski.M , *Electrical and photovoltaic properties of ZnO/Si heterostructures with ZnO films grown by atomic layer deposition*, Thin Solid Films 563(2014), 28–31. https://doi.org/10.1016/j.tsf.2013.10.110.

[12] Yakuphanoglu. Fahrettin, Caglar. Yasemin, Caglar. Mujdat, and Ilican. Saliha, *ZnO/p-Si heterojunction photodiode by sol–gel deposition of nanostructure n-ZnO film on p-Si substrate*, Materials Science in Semiconductor Processing 13(2010), 137–140. https://doi.org/10.1016/j.mssp.2010.05.005.

[13] He. Guan-ru, Lin. Yow-jon, Chang. Hsing-cheng and Chen. Ya-hui, *Effects of interface modification by $H_2O_2$ treatment on the electrical properties of n-type ZnO/p-type Si diodes*, Thin Solid Films 525(2012), 154–157. https://doi.org/10.1016/j.tsf.2012.10.056.

[14] Schmitsdorf. R.F., Kampen. T.U.,M¨onch.W. , *Explanation of the linear correlation between barrier heights and ideality factors of real metal-semiconductor contacts by laterally nonuniform Schottky barriers*, Journal of Vacuum Science and Technology B: Microelectronics and Nanometer Structures 15(1997), 1221–1226. https://doi.org/10.1116/1.589442.

[15] Aksoy. Seval and Caglar. Yasemin, *Effect of ambient temperature on electrical properties of nanostructure n-ZnO/p-Si heterojunction diode*, Superlattices and Microstructures 51(2012), 613–625. https://doi.org/10.1016/j.spmi.2012.02.018.

[16] Klason. P, Rahman. M. M, Hu. Q, Nur. O, Turan. R and Willander. M, *Fabrication and characterization of p-Si/n-ZnO heterostructured junctions*, Microelectronics Journal 40(2009), 706–710. https://doi.org/10.1016/j.mejo.2008.07.070.